DOI: https://doi.org/10.36499/jim.v21i1.12682

NUMERICAL INVESTIGATION OF THE EFFECT OF FIN THICKNESS ON STRAIGHT FIN HEAT SINK ON HEAT TRANSFER PERFORMANCE

Muhamad Safi'i[1*], Nazaruddin Sinaga[2], Tabah Priangkoso[3], Suheri Suheri[4], Rouf Muhammad[5]

[1]Departement of Mechanical Engineering, Faculty of Engineering and Computer Science, Sains Al Qur'an University.
Jl. KH. Hasyim Asy'ari Km. 03 Kalibeber, Kec. Mojotengah, Kab. Wonosobo 56351.
[2*] Departement of Mechanical Engineering, Faculty of Engineering, Diponegoro University.
Jl. Prof. Soedarto, S.H, Tembalang, Kota Semarang, Jawa Tengah, 50275.
[3] Departement of Mechanical Engineering, Faculty of Engineering, Wahid Hasyim University.
Jl. Menoreh Tengah X/22, Sampangan, Semarang 50236.
[4] Departement of Mechanical Engineering, Faculty of Engineering, Samudera University.
Jl, Prof. Dr. Syarief Thayeb, Meurandeh, Langsa Lama, Kota Langsa, Aceh 24416.
[5] Departement of Mechanical Engineering, Faculty of Engineering, State Polytechnic of Jakarta PSDKU Demak.
Jl. Sultan Trenggono No.61, Katonsari, Kec. Demak, Kabupaten Demak, Jawa Tengah 59516.

[*]Email: muhamadsafii17@unsiq.ac.id.

Abstrak

The heat load on computer chips during computing performance is the main topic, so a cooling device is needed. Heat sink is one of the tools commonly applied to reduce the heat load during computing performance of computer systems. Various heat sink configurations have been widely developed and studied to achieve designs with optimal thermal performance. This research was conducted to investigate the best design on a straight fin heat sink (SFHS) that has the best thermal and hydraulic performance. SFHS with fin thickness variations of 1 mm, 2 mm, and 3 mm are proposed in this study. The numerical method was carried out using the Computational Fluid Dynamics program by considering fluid flow velocities of 4 m/s, 6 m/s, 8 m/s, and 10 m/s. The numerical results show that the cooling rate of SFHS can be increased by using SFHS with a thickness of 3 mm and a fluid flow velocity of 10 m/s, with a maximum Nusselt number value of 59.74. Therefore, it is concluded that the SFHS has prospects for further study and can be applied practically in the field for microelectronic components and computer systems.

***Keywords**: Heat sink, SFHS, Straight fin.*

INTRODUCTION

The increase in computing work and chip penetration in computer systems are the main factors causing heat generation, so cooling is needed (Yifan. Li et al., 2025). An effective and efficient cooling device is a solution to overcome the problem of heat load on computer systems (Sherin. M et al., 2025). In this case, a heat sink is the right cooling tool to use because it can reduce the heat load effectively and efficiently (John. S. S et al, 2025, Yongrui. B et al, 2025). *Electrical chip*, CPU computer, LED of light, and Li-ion battery, is an examples of electronic devices that are cooled using a heat sink. (Moradikazarouni. A et al., 2019, Pan. M et al., 2021, and John. S. S et al, 2025).

Fanless heat sinks are very common in thermal applications found in electronic devices because they are compact, quiet, and do not require much power consumption in their operation (Mohamed. H et al., 2025). The free convection method is often used in heat sink applications because the intensification of fluid flow and thermal distribution shows a more pronounced heat absorption gradient (Hussein, S. S., et al, 2024 and Ishtiaque H. M. D., 2025). In addition, the forced convection method can be applied to quickly remove heat load (Anas. A et al., 2024). The efficiency and performance of heat sinks are continuously being developed and studied to optimize the performance of electronic devices (Alihoseini. Y et al., 2021 and Song. J. G et al., 2021).

Various ideas and proposals for heat sink geometry configurations have been developed. However, the oblique type heat sink is still the best at this time (Kanargi. B et al., 2020, and Safi'i. M et al., 2022). The oblique type heat sink provides good heat transfer performance data, but the difficulty in the production process and maintenance are problems that need to be reviewed so that they can be applied to practical cooling applications in the field for micro electronic components

(Alihosseini. Y et al, 2020, Kanargi. B et al., 2020, and Safi'i. M et al., 2022). SFHS is interesting to discuss and develop because of its reliability (Safi'i. M et al., 2024). The reasons for the ease of formation, production, maintenance and repair make SFHS popular with many technicians (Yifan. L et al., 2025 and John. S. S et al, 2025). SFHS integration has been shown to increase pumping power and reduce thermal resistance (Anas. A et al., 2024).

There has been a lot of research, both experimental and numerical, to characterize the thermal and hydraulic performance of SFHS (Refaey. H. A et al., 2023). 3 SFHS models with different fin configurations, namely types A, B, and C, were studied using experimental and numerical methods by considering free convection operations and varying the fin heights of 70 mm, 75 mm, and 80 mm. The results showed that SFHS with models A, B, and C each had good thermal performance with evidence that the thermal resistance could be reduced by 5.7% for type A, 14.4% for type B, and 15.6% for type C, confirming that the acoustic size of SFHS affects heat transfer performance (Huang. C. H and Chen. W. Y et al., 2022). SFHS in solar panel cooling applications was studied using an experimental approach by considering variations in the incoming heat flux of 0.9955 W/cm², 1.107 W/cm², 1.326 W/cm², and 2.16 W/cm². The results showed that variations in the incoming heat flux provided thermal performance data as evidenced by a decrease in the surface temperature of the solar panel by 4% (Rafey. H. A et al., 2022).

SFHS with grooved and non-grooved diamond fin shapes were studied using an experimental method by considering variations in the geometric aspect ratio of 8;1 to a constant fin length and thickness of 1600µm. As a result, the heat sink with grooved diamond fins has the most optimum performance compared to the heat sink with non-grooved diamond fins (Jianley. C et al., 2024). Experimental and numerical studies on SFHS with aluminum material types AL-6061 and AL-6062 were conducted. The results showed that SFHS with aluminum material type AL-6062 had the largest PEC value with a value of 5 (Ehtesham. A et al., 2024).

SFHS is characterized by a numerical approach, a viscous model variation, a solution method, and a number of grid meshes are proposed in this study. The research results show that the variation of the number of grids by 931,900 with the Realizable k-ε viscous model and coupled solution method can reduce the fin surface heat load by 20% (Safi'i, M et al., 2024). SFHS arranged in V and X shapes were studied using numerical methods at variations in fluid mass flow rates of 0.001 kg/s-0.005 kg/s. The results showed that the heat sink with an X-shaped arrangement had good cooling performance, as evidenced by an increase in the Nusselt number of 27.6%. (Jin. Y et al., 2025). The inline heat sink was tested by experimental and numerical methods. The Reynolds number variation of 100-700 was proposed in the study. As a result, the Nusselt number value can be increased by 80%-91% (Nedal O. E. S et al., 2025).

Previous research focused on the flow that develops thermally and hydrodynamically against fin shape, Reynolds number, fluid flow velocity, incoming heat flux, fin size, and material type. In addition, there is no numerical study of the effect of fin thickness and fluid flow velocity on fluid flow and heat transfer. Therefore, research was conducted to determine the effect on thermal and hydraulic performance numerically using the Computational Fluid Dynamics computer program by selecting Transition SST k-ω as the viscous model.

METHOD

Physical Model

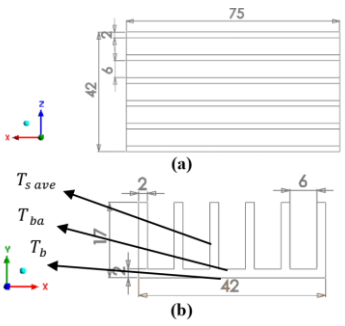

Figure 1. (a) Top view of SFHS, (b) Front view of SFHS.

DOI: https://doi.org/10.36499/jim.v21i1.12682

Figure 1 (a) and (b) are the top and front views of the SFHS along with its dimensions. The data collection locations are indicated by arrow lines for Temperature bottom (Tb), Temperature base (Tba), and Temperature average of fins (Ts ave). SFHS modeling was performed using Solidworks drawing software and referring to the literature. (Adhikari. R. C et al., 2020) and SFHS is modified by considering fin thicknesses of 1 mm, 2 mm, and 3 mm.

SFHS Design

The novelty of this research is the modification of the SFHS based on the literature (Adhikari. R. C et al., 2020) to SFHS with fin thickness variations of 1 mm, 2 mm, and 3 mm and fluid flow velocities of 4 m/s, 6 m/s, and 8 m/s. The supporting size variables are determined for fin geometry L_{ch} 75 mm, W_{hs} 42 mm, W_{ch} 6 mm, H 17 mm as described by Figure 1 (a) and (b).

Numerical Study

Computational Domain

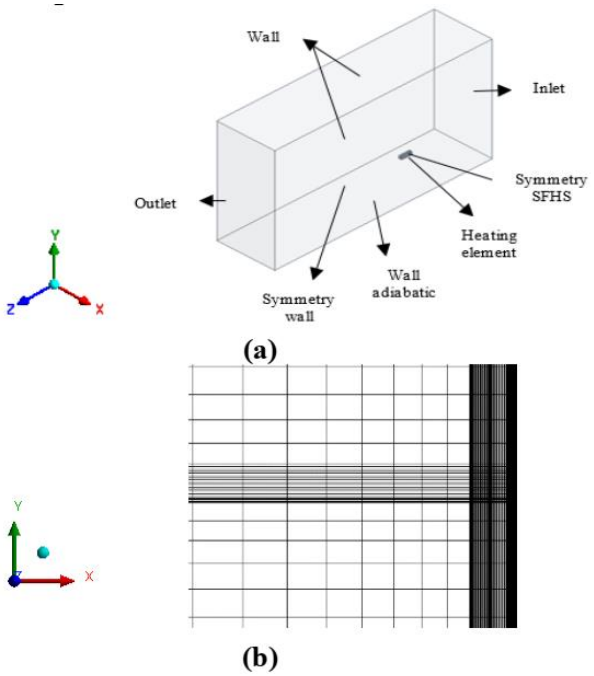

Figure 2. (a) Computational Domain and Boundary Condition Determination, (b) Tetrahedral Grid Structure.

The SFHS computational domain is determined with a size of 750 mm x 400 mm x 400 mm, and the symmetry operation is chosen because it considers efficiency and durability when the computation is running. The determination of the location of the boundary conditions is explained in Figure 2 (a) numerical study of single-phase flow through fins with steady state. The volume control technique is applied to the meshing process to discretize the differential equations with a second-order upwind scheme for better accuracy and results. The structure and high resolution of the multizone mesh are applied because it considers the geometry of the solid and fluid parts in the computational domain. In addition, this method is carried out to capture the effects of thermal and hydraulic boundary layers more accurately, as explained in Figure 2. (b).

The continuity, momentum, and energy equations during numerical studies using the free convection method on square groove SFHS are shown by equations 1, 2, 3, 4, and 5:

Continuity equation:

$$\frac{\partial u}{\partial x}+\frac{\partial v}{\partial y}+\frac{\partial w}{\partial z}=0 \quad (1)$$

Where T_s ave is the average temperature of the heat sink fins, and the bottom surface of the heat sink experiences a constant heat flux.

Momentum equation:

$$\rho\left(\frac{\partial u}{\partial x}+\frac{\partial uv}{\partial y}+\frac{\partial uw}{\partial z}\right)=\frac{\partial P}{\partial x}+\mu\left(\frac{\partial^2 u}{\partial x^2}+\frac{\partial^2 u}{\partial y^2}+\frac{\partial^2 u}{\partial z^2}\right) \quad (2)$$

$$\rho\left(\frac{\partial uv}{\partial x}+\frac{\partial v^2}{\partial y}+\frac{\partial vw}{\partial z}\right)=-\frac{\partial P}{\partial x}+\mu\left(\frac{\partial^2 v}{\partial x^2}+\frac{\partial^2 v}{\partial y^2}+\frac{\partial^2 v}{\partial z^2}\right) \quad (3)$$

$$\rho\left(\frac{\partial uw}{\partial x}+\frac{\partial uw}{\partial y}+\frac{\partial uw^2}{\partial z}\right)=-\frac{\partial P}{\partial x}+\mu\left(\frac{\partial^2 w}{\partial x^2}+\frac{\partial^2 w}{\partial y^2}+\frac{\partial^2 w}{\partial z^2}\right)+g(\rho-\rho_\infty) \quad (4)$$

Energy equation:

$$\rho\left(\frac{\partial uT_a}{\partial x}+\frac{\partial vT_a}{\partial y}+\frac{\partial wT_a}{\partial z}\right)=-\frac{k}{C_p}+\mu\left(\frac{\partial^2 T_a}{\partial x^2}+\frac{\partial^2 T_a}{\partial y^2}+\frac{\partial^2 T_a}{\partial z^2}\right) \quad (5)$$

Grid Independent Test

Independent grid tests were conducted to determine the optimum point of the experimental values in the form of Temperature bottom (T_b) calculated on the bottom grooved SFHS section, Temperature bottom (T_{ba}) calculated on the bottom surface of the SFHS, while the average temperature of fins (Ts ave) was calculated on all surfaces of the SFHS fins. To ensure that the computational domain is adequately completed and the numerical error is small, an independent grid test was conducted with the aim of gradually refining the grid size until acceptable convergence is achieved for the maximum fin temperature. The independent grid test on the SFHS was conducted by considering the number of mesh cells in the computational domain between 135210, 241350, 337200, and 441500. In addition, the fluid flow velocity and constant heat flux were also considered in this grid test. The results of the independent grid test are presented in the graph in Figure 3. The relationship between grid number and heat transfer coefficient value. Calculations on numerical studies in grid tests show that the relative error between grids 135210 and 241350 is ±1.1%, 241350 and 337200 is ±1.02%, while 337200 and 441500 is ±0.3%.

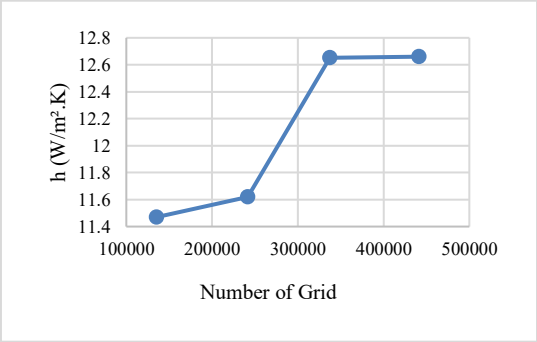

Figure 3. Relationship between Number of Grids and Heat Transfer Coefficient..

Set up

The modeling and computational domain are created by considering experiments from the literature (Adhikari. R. C et al., 2020). Constant thermal physical properties and forced convection methods are applied in this research. Steady air flow conditions are assumed to characterize the convective heat transfer between the SFHS interfaces. Convergence criteria 10^{-4} for flow, and 10^{-7} for energy used. The air fluid used as a coolant in this numerical study has material properties of density ρ = 1,2096 kg/m³, specific heat C_p = 1005 J/kg.K, viscosity μ = 1,915×10^{-5} kg/ms, thermal conductivity k = 0,0261 W/m.K, and molecular weight 28,966 kg/kmol assuming a basic ambient temperature of 25°C. Aluminum alloy 6062 is used for the heat sink module, and the thermal conductivity is assumed to be k = 168 (W/m.K) with Q = 4,71 W. Non-slip walls are applied to the fin surfaces specified in the boundary conditions.

DOI: https://doi.org/10.36499/jim.v21i1.12682

Numerical Data Reduction

The operating conditions of the SFHS simulation refer to the inlet to outlet air flow direction on the vertical axis of the ZX CFD Software, and the Reynolds number is defined by equation 6:

$$R_e = \frac{\rho.V.Dh}{\mu} \quad (6)$$

The hydraulic diameter is defined by the equation 7:

$$D_h = \frac{4s.H}{2(H.s)} \quad (7)$$

The surface area of SFHS is calculated by the equation 8:

$$A = (nLH)+(PL) \quad (8)$$

The SFHS base area is calculated using equation 9:

$$Ab = 2(LP) \quad (9)$$

The heat transfer coefficient can be calculated using equation 10:

$$h = \frac{Q}{A_b(T_{s\,ave} - T_\infty)} \quad (10)$$

The Nusselt number is defined to compare the values between convection and conduction heat transfer, which can be calculated using equation 11:

$$Nu = \frac{h.L}{K} \quad (11)$$

RESULT AND DISCUSSION

Validation

Validation was carried out through a numerical approach to experiments conducted in the literature. (Adhikari. R. C et al., 2020) In SFHS with the forced convection method, the parameters to be sought in this study are the parameters T_b, T_{ba}, $T_{s\,ave}$ in order to determine the value of the heat transfer coefficient and Nusselt number in the newly proposed SFHS. Validation is carried out by varying the Reynolds number against the constant geometric parameter values of the basic SFHS presented in Figure 4, the relationship between grid number and Nusselt number.

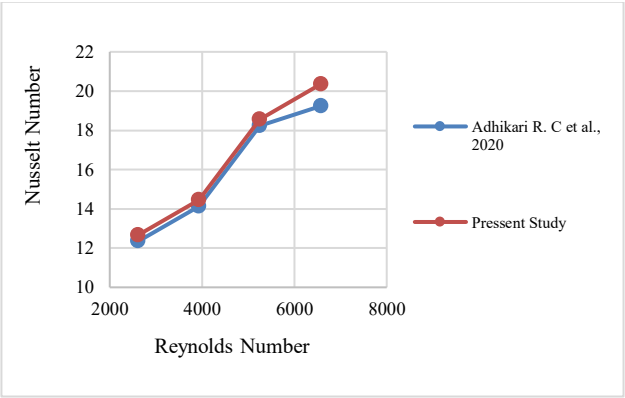

Figure 4. Relationship between Reynolds Number and Nusselt Number.

In the graph, you can see the results of experiments by literature (Adhikari. R. C et al., 2020). In SFHS, the Nusselt number value was obtained as 19.24. Meanwhile, the simulation results for the

experiment from the literature obtained a Nusselt number of 20.36, with the smallest relative error being 1.77% and the largest being 2.5%. These results indicate a good agreement between the experiments (Adhikari. R. C et al., 2020) to the numerical studies being validated.

Heat Transfer Characteristics of SFHS

Optimization of SFHS with variations in fin thickness at various fluid flow rates is carried out to find the most optimal SFHS design. The heat transfer coefficient has a strong relationship to the incoming heat flux in the SFHS. We assume the incoming heat flux is constant at 4.71 W. In the literature experiment (Adhikari. R. C et al., 2020), the heat transfer coefficient value is calculated based on the average temperature value of the SFHS fin surface. This value is taken when the SFHS is in a steady state, so that the distribution of the fin surface temperature is even. The thickness of the fin also has a fairly strong effect on the heat transfer coefficient because the acoustic size of the fin allows the heat dissipation area to work effectively. This influence increases with the increase in the fin thickness dimension and fluid flow velocity.

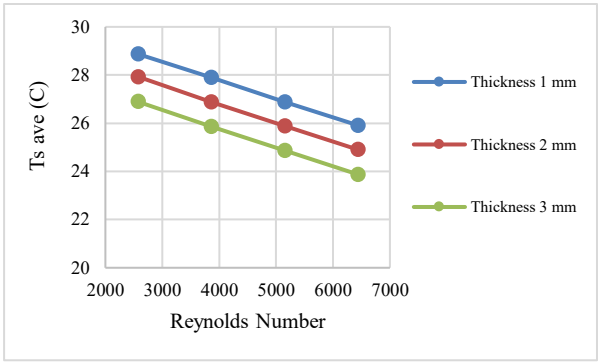

Figure 5. Relationship between Reynolds Number and Average Fin Surface Temperature.

Figure 5 shows a graph of the relationship between Reynolds number and the average temperature of the fin surface. ($T_{s\ ave}$) on the SFHS. The average temperature of the fin surface ($T_{s\ ave}$) is the value used to calculate the heat transfer coefficient value. With the same operating conditions, the temperature value tends to decrease slowly between 1ºC to 2ºC in each variation of fin thickness. SFHS fin thickness of 3 mm has good heat transfer performance in this investigation, as evidenced by the increase in Reynolds number, the average temperature of the fin surface tends to decrease slowly, but it is different for SFHS with a fin thickness of 1 mm, although it has a good temperature decrease trend, The effect of the 1 mm thick fin dimension is not yet able to provide good thermal performance.

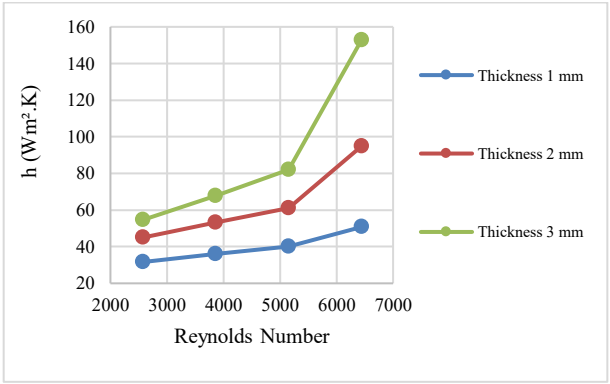

Figure 6. Relationship between Reynolds Number and Heat Transfer Coefficient.

Figure 6 is a graph of the relationship between Reynolds number and the heat transfer coefficient value of SFHS. The best value is generally obtained in SFHS with a fin thickness of 3

DOI: https://doi.org/10.36499/jim.v21i1.12682

mm, the smallest heat transfer coefficient value is obtained in SFHS with a fin thickness of 1 mm with a value 31,63 W.m^{2}K, while the largest was obtained in SFHS with a fin thickness of 3 mm with a value of 54,66 W.m^{2}K varied the same Reynolds number. In SFHS with fin thicknesses of 1 mm and 2 mm the distribution of incoming air flow tends to vary, resulting in less than optimal heat absorption from the heating element. The size of the fin thickness may affect heat absorption; the small fin thickness is proven to be less effective in absorbing heat, so that by increasing the fin thickness, it is expected that the SFHS can work optimally. However, the constraints of acoustic size for applications in computer systems are the main problem; therefore, the importance of design optimization and simulation in finding the optimal design on SFHS.

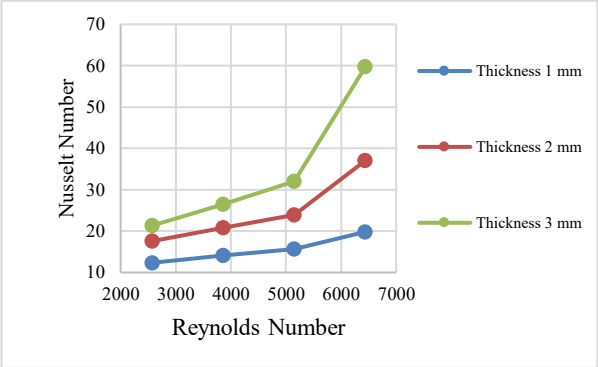

Gambar 7. Hubungan Bilangan Reynolds dan Koefisien Perpindahan Panas.

The decrease in the surface temperature of the SFHS fin plays a major role in increasing the Nusselt number. The Nusselt number is defined as the ratio between convection heat transfer and conduction heat transfer that occurs in the SFHS. Figure 6 shows a graph of the relationship between the Reynolds number and the Nusselt number in the SFHS. The highest Nusselt number occurs in the SFHS with a fin thickness variation of 3 mm, with a value of 59.74 at a fluid flow velocity of 10 m/s, while with the same variation, the Nusselt number is only around 19.83. These results confirm that increasing the variation in thickness and fluid flow velocity can significantly increase the Nusselt number value.

Effect of Fin Thickness

Numerical investigation on SFHS with fin thickness variation of 1 mm, 2 mm, and 3 mm is characterized at various fluid flow velocities. The goal is to optimize the best SFHS design to be proposed in a practical application in the field. In addition, a numerical investigation of SFHS with fin thickness variation is carried out the aim whether the proposal can reduce the base temperature of SFHS. Generally, the thickness of SFHS fins affects the strength, stability, and acoustic weight of SFHS. In addition, a good SFHS temperature reduction is the main goal of this investigation.

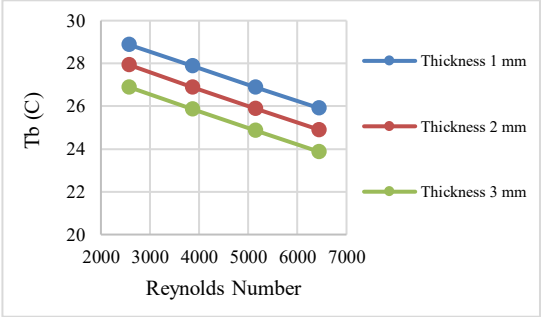

Figure 8. Relationship between Reynolds Number and Temperature of the Bottom Part of the SFHS.

In each step of the SFHS design is solved by the forced convection numerical method is used to find the optimal value of the SFHS, and only effective design variables are considered to optimize

its performance. The thickness of the fin allows for increased heat absorption, this is because the heat dissipation area also increases. As a result, thermal conductivity can be increased slowly and allowing the effectiveness of the SFHS to be optimal. The use of this fin thickness can also increase its large surface area, which is useful for emitting heat to the surrounding air, so that component cooling is more effective.

Figure 8 explains the relationship between the Reynolds number and the lowest surface temperature value of the SFHS. (T_b), The temperature value ranges between 28,87°C-25,91°C at a fin thickness variation of 1 mm, 27,93°C-24,90°C at a fin thickness variation of 2 mm, dan 26,89°C-23,87°C on 23.87 °C at a fin thickness of 3 mm in various variations of fluid flow speed. The results confirmed that the magnitude of the fin thickness affects the value of the lower surface temperature of the SFHS (Tb). The thickness of the fin on the SFHS plays an important role in the dissipation of heat on the fin surface to the surrounding air, so that the heat transfer capacity is also large. However, in contrast, if the fin thickness is small, heat dissipation becomes slow, this is due to the small fin gap structure causes the air flow to be obstructed, so that heat is often trapped around the fin.

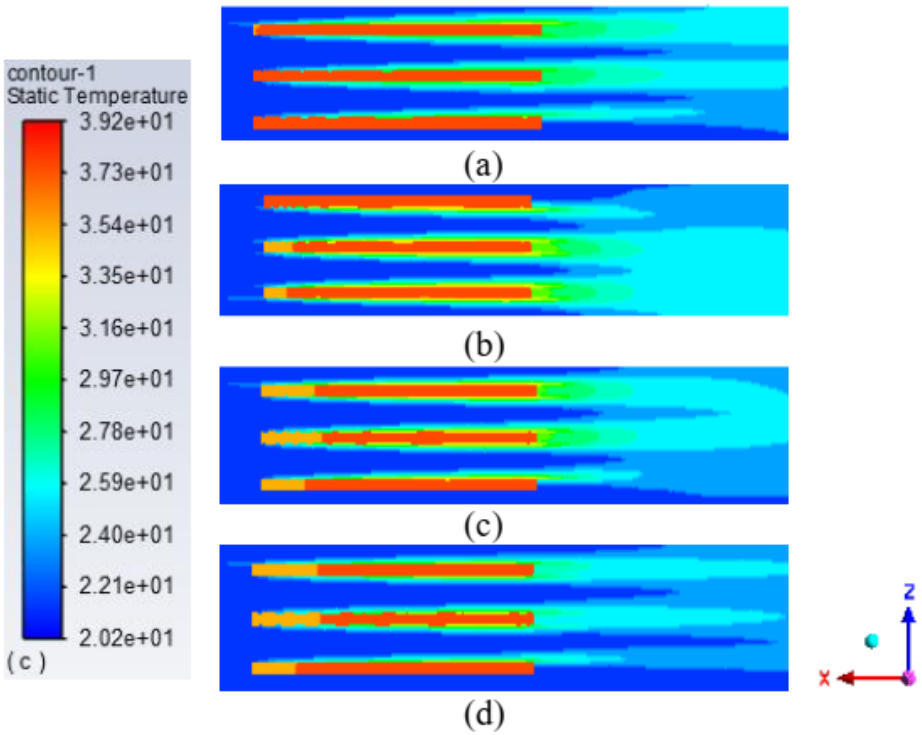

Figure 9. (a, b, c, and d) SFHS Temperature Contours t = 3 mm X-Z Plane Direction Height Y = 5 mm from Heating Element at v = 4 m/s, 6 m/s, 8 m/s, and 10 m/s.

Figure 9 a, b, c, and d are the temperature contours resulting from numerical investigations on SFHS with a fin thickness of 3 mm at various air flow velocities and with a constant incoming heat flux of 4.71 W taken on the XZ axis with a height of Y = 5 mm from the SFHS surface. The temperature distribution around the fin surface tends to be even. The fin with a high temperature is slowly swept by the fluid flow, which allows slow cooling around the fin. The magnitude of the variation in fin thickness and fluid flow velocity proves that the difference in fin surface temperature is more real.

Even with the same operating conditions and fin thickness variations, in fact the magnitude of the fluid flow velocity variation proves that the temperature change pattern around the fin tends to be different, initially the SFHS with heat provided by the heating element tends to be red, but slowly turns orange when the air flow develops around the fin. It is possible that the temperature contour of the fin surface tends to be even with the same color if the operating conditions are already in a steady state. The temperature difference varies greatly in each variation of fluid flow velocity; the temperature difference from the results of numerical studies ranges from 2ºC to 4ºC. This

DOI: https://doi.org/10.36499/jim.v21i1.12682

difference shows that the optimization work of SFHS with variations in fin thickness at various fluid flow velocities works well, so that these results are expected to be applied directly in the field.

Effect of Flow Velocity Variations

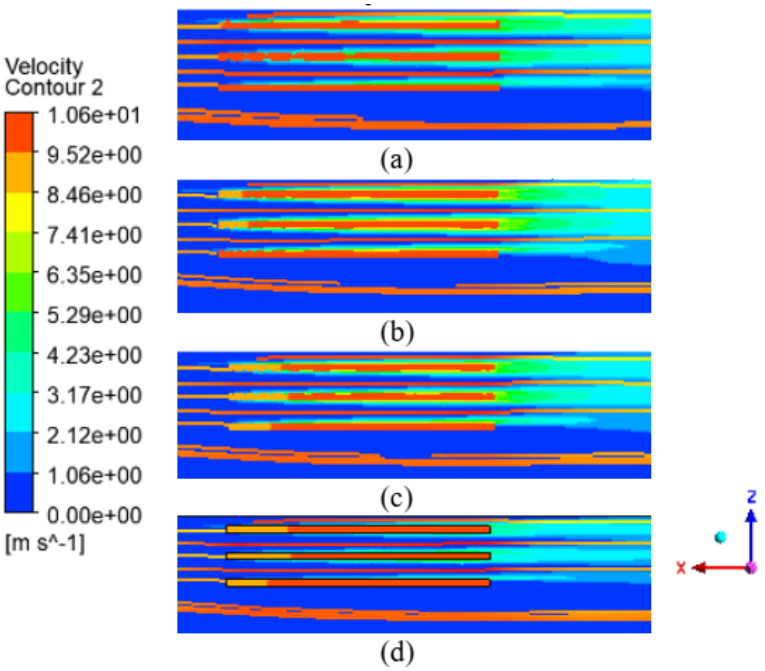

Figure 10. (a, b, c, and d) Streamline Contour of SFHS t = 3 mm X-Z Plane Direction Height Y = 5 mm from Heating Element at v = 4 m/s, 6 m/s, 8 m/s, and 10 m/s.

In general, the airflow velocity around the SFHS gap is higher compared to other parts because the inlet area and airflow field are larger, allowing low-temperature air to enter freely. Figure 10a, b, c, and d show the temperature contours resulting from numerical investigations on SFHS with a fin thickness of 3 mm at various airflow velocities and with a constant incoming heat flux of 4.71 W taken on the XZ axis with a height of Y = 5 mm from the SFHS surface. Visualization of the distribution and characteristics of the fluid flow that develops around the SFHS shows that there is a tendency for fluid behavior to be the same. The developing flow initially shows laminar flow characteristics, then when the flow reaches the front of the SFHS and because of the geometric effect of the SFHS, there is a collision force that occurs. The collision force allows the fluid behavior to change from laminar to transition. In this situation, the characteristics of the fluid flow tend to form small vortex patterns with not too much intensity. Based on the numerical results, it is known that the characteristics of the fluid flow do not show significant differences even though the variation of the fluid flow velocity and the variation of the SFHS fin thickness are increased. The average velocity of the fluid flow that develops around the SFHS fin tends to be uniform, namely with a value between 7 m/s and 8.5 m/s.

In addition, the distribution of the developing pressure is also influenced by the properties of the fluid and the intensity of the fluid. On the inlet side, the local fluid pressure tends not to be visible. However, strangely, around the middle of the SFHS, the free stream fluid pressure tends to be real and shows a variety of gradients; in addition, the contour of the hydraulic boundary layer distribution in this case also accommodates the pressure in various parts of the test. This may be due to the meeting of the heat field and air passing through the SFHS gap, so that the fluid pressure tends to increase slowly. In addition, the magnitude of the variation in fluid flow velocity also plays an important role in increasing fluid pressure. As a result, the pumping power also tends to be large. However, this phenomenon is also slightly beneficial to the cooling effect of the SFHS.

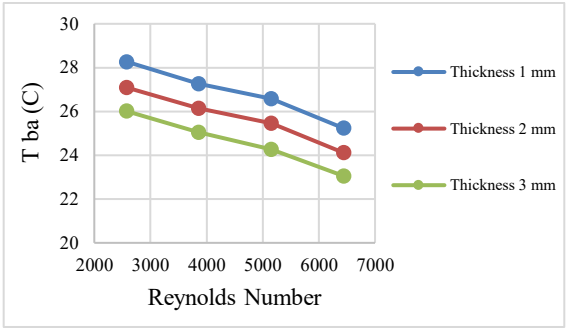

Gambar 11. Hubungan Bilangan Reynolds dan Temperatur Permukaan Bawah SFHS.

Figure 11 explains the relationship between the Reynolds number and the SFHS bottom surface temperature (T_{ba}). The temperature values range from 28.12°C-25.02°C at a fin thickness variation of 1 mm, 27.14°C-24.10°C at a fin thickness variation of 2 mm, and 26.14°C-23.06°C. At large fin thicknesses, the average temperature has a trend to grow with a significant decrease in the fin surface temperature. In addition, the thin thermal boundary layer around the SFHS fins shows a decrease in the temperature gradient. It is possible that by adding variations in fin thickness to the SFHS, better cooling is possible. However, the problem is that the acoustic size of the SFHS must adjust to the dimensions of the micro-electronic components on the computer device, so that increasing the fin thickness does not necessarily become the main choice and alternative to cool electronic components. In the research we have studied, the results prove that the effect of air flow speed variation greatly affects thermal performance. These results allow for recommendations to be applied in practical applications such as computers, solar cells, and the latest is cooling in car AC installations.

CONCLUSION

The results of the numerical study show that the cooling rate of SFHS can be increased by varying the fin thickness and fluid flow velocity. Therefore, it can be concluded that a fin thickness of 3 mm and a fluid flow velocity of 10 m/s have prospects for further research and are prospective for practical application in the field of micro-electronic components and computers due to the increase in the Nusselt number with a maximum value of 59.74.

Competing Interest Statement

The authors declare that they are not aware of any competing financial interests or personal relationships that might have appeared to influence the work reported in this paper.

Acknowledgements

Beasiswa Pendidikan Indonesia (BPI). Building C Lantai 13 Jl. Jenderal Sudirman Senayan, Jakarta 10270.

Energy Efficiency and Conservation Laboratory, Diponegoro University. Jl. Prof. Sudarto No.13, Tembalang, Semarang, Central Java (50275), Indonesia.

CFD Research Group Sains Al Qur'an University. Jl. KH. Hasyim Asy'ari Km. 03 Kalibeber, Kec. Mojotengah, Kab. Wonosobo 56351.

REFERENCES

Yifan L., Congzhe Z., Guodong X., (2025). Experimental investigation on the Phase Change Liquid Cooling Characteristics in the Offset Grooved Microchannel Heat Sink. *Applied Thermal Engineering*. 269(1), 1-14.

Sherin. M., Gaosheng. W., Hoosam A. M. El-Hamid., (2025) Multi-Objective Optimization of Grooved Circular Pin-Finned Heat Sink with Phase Change Material. *Applied Thermal Engineering*. 262(2), 1-12.

John. S. S., Ravikiran C., Bridjesh. P., Seshibe M., (2025). Novel Design of Serpentine Channel Heat

DOI: https://doi.org/10.36499/jim.v21i1.12682

Sinks with Rectangular and Triangular Ribs and Grooves for 25Ah Li-Ion Battery Thermal Management. *International Journal of Thermofluids*. 25(1), 1-18.

Yongrui. B., Zhen. C., Zhenzhou. L., Yuxiang L., Yuetong L., Xu Lu., Ding Y., Zhenfei F., (2025). Experimental Investigation on the Effects of Inclined Grooves on Flow Boiling Heat Transfer and Instability in a Minichannel Heat Sink. *International Journal of Heat and Mass Transfer*. 236(2), 1-13.

Safi'i, M., Sinaga, N., Syaiful, & Sukiman. (2022). Computational Study of the Effect of Fin Longitudinal Spacing and Reynolds Number on the Performance of Oblique Heat Sinks. *International Research Journal of Innovations in Engineering and Technology (IRJIET)*, 6(9), 27-38.

Safi'i, M., Sinaga, N., Priangkoso, T., Susanto, S., & Digdoyo, A. (2024). Investigasi Model Numerik pada Simulasi Heat Sink Sirip Lurus Dengan Memvariasikan Jumlah Grid, Model Viscous dan Metode Pemecahan dengan Pendinginan Konveksi Bebas. *Jurnal Ilmiah Momentum*, 20(1), 31-41.

Huang. C. H and Chen W. Y., (2022). *A* Natural Convection Horizontal Straight-Fin Heat Sink Design Problem To Enhance Heat Dissipation Performance. *International Journal Thermal Science*, 176(2), 1-13.

Moradikazerouni. A, Afrand. M, Alsarraf. J, Wongwises. S, Asadi. A, and Nguyen. T. K. (2019). Investigation of a Computer CPU Heat Sink Under Laminar Forced Convection using a Structural Stability Method. International *Journal Heat and Mass Transfer*. 134(3), 1218–1226.

Pan. M, Chen. Z, and Li C. (2021). Experiment and Simulation analysis of Oriented Cut Copper Fibre Heat Sink for LED Water Cooling," Ca*se Study Thermal Engineering*. 24(4), 1- 17.

Mohamed. H., Roberta. P., Ahmed E., Jason D., Roger K., (205) A Lightweight Additively Manufactured Two-Phase Integrated Natural Convection Heat Sink. *Applied Thermal Engineering.*

Hussein S. S., Khalid B. Saleem., Badr. M. A., Mohamed T., Abdelkarim A., Lioua K., (2024). Numerical Investigation of Natural Convection From a Horizontal Heat Sink with an Array of Rectangular Fins. *Case Studies in Thermal Engineering*. 61(4), 1-16.

Ishtiaque H. M. D., Samiul H. C., Syed S. U. Ahmed., Abu Hamja., Istiaq J. S., (2025). Forced Convective Heat Transfer Over Twisted and Perforated Forked Pin Fin Heat Sink: a Numerical Study. *International Journal of Thermal Sciences*. 211(1), 1-15.

Alihosseini. Y., Targhi. M. Z., and Heyhat. M. H., (2020). Thermohydraulic Performance of Wavy Microchannel Heat Sink with Oblique Grooved Finned. *Applied Thermal Engineering*. 189(2), 1-11.

Song. J. G., Lee. J. H., and Park. I. S., (2021). Enhancement of the cooling Performance of Naval Combat Management System using Heat Pipe. *Applied Thermal Engineering*. 188(2), 1-12.

Alihosseini. Y., Targhi. M. Z,, and Heyhat. M. H., (2020). Thermohydraulic Performance of Wavy Microchannel Heat Sink with Oblique Grooved Finned. *Applied Thermal Engineering*. 189(2), 1-11.

Kanargi. B., Tan. J. M. S., Lee. P. S., and Yap. C., (2020). A Tapered Inlet/Outlet Flow Manifold for Planar, Air-Cooled Oblique Finned Heat Sinks. *Applied Thermal Engineering*. 174(1), 1-18.

Ehtesham. A., Sajan T., Jaehyun. P., Jaemun. C., Jaehun. C., Chanwoo. P., Hesung. P., (2024). A Novel Spiral Grooved Cooling Path Heat Sink for the Cooling of High Voltage Direct Current Devices. *International Journal of Thermal Sciences*. 195(3), 1-16.

Anas. A., Fadi. A., Bobby. M., (2024). Characterization of MEMS Heat Sinks Having Straight Microchannels Integrating Square Pin-Fins for Liquid Cooling of Microelectronic Chips. T*hermal Science and Engineering Progress*. 45(4), 1-15.

Refaey. H. A., Mathkar A. A., Samir. B., Said. G. K., Mohamed. E., Abdelrahman. M. A., (2023). An Experimental Investigation on Passive Cooling of a Triple-Junction Solar Cell at High Concentrations Using Various Straight-Finned Heat Sink Configurations. *Case Studies in Thermal Engineering*. 51(2), 1-17.

Nedal. O. E. S., Fadi. A., Bee. T. C., Bobby. M., (2025). Performance Evaluation of MEMS Heat Sinks Having Straight Microchannels Integrating Rectangular Sidewall Cavities in In-Line Pattern. *Applied Thermal Engineering*. 266(1), 1-16.

Jin. Y., Yongfeng. Q., Ningkang. D., Liang. D., Wenbo. H., Xiaofan. Z., Shengli. W., Hongxing. W., (2023). Three-Dimensional Numerical Investigation of Flow and Heat Transfer Performances of Novel Straight Microchannel Heat Sinks. *Diamond and Related Materials*. 140(1), 1-18.

Jianlei. C., Haozhe. K., Jian. D., Xiangyang. D., Zhijun. W., Zhengjie. F., Wenjun. W., Xuesong. M., (2024). High-Quality Fabrication of Diamond Straight Microchannels Heat Sink with Large Aspect Ratio Microchannels using UV Nanosecond Laser Based On Multi-Feed Method. *Optics & Laser Technology*. 171(2), 1-18.

Adhikari. R. C., Wood. D. H., Pahlevani. M., (2020). An Experimental and Numerical Study of Forced Convection Heat Transfer from Rectangular Fins at Low Reynolds Numbers. *International Journal of Heat and Mass Transfer*. 163(3), 1-12.